



A New Methodology to Describe Non-Linear Characterization Depending on Temperature of a Semi-Active Absorber Based on Bouc-Wen Model

Zekeriya PARLAK^{1,*} , M. Erturk SOYLEMEZ² , Ismail SAHIN³ 

¹Sakarya University, Faculty of Engineering, Department of Mechanical Engineering, Sakarya/Turkey

²Muş Alparslan University, Faculty of Engineering, Department of Mechanical Engineering, Muş/TURKEY

³Sakarya University of Applied Science, Vocational School of Arifiye, /Turkey

Highlights

- A new methodology to describe dynamic behaviours of MR absorber depending on temperature.
- Bouc-Wen model for temperature changing.
- The damper force defined depending on temperature with a single equation.
- Control comfortably and more stability MR absorber on a structure, vehicle, and medical haptic.
- The rheological test of MR fluid and MR absorber tests under different temperature conditions.

Article Info

Received: 30 Apr 2021
Accepted: 22 Dec 2021

Keywords

MR Damper
Dynamic model
Bouc-Wen model
Hysteresis behaviours
Temperature

Abstract

The nonlinear behavior of semi-active magneto-rheological (MR) absorbers should be described for improving control algorithms. Also, overheating in the working conditions of the MR absorber due to current excitation and high damping velocity seriously changes the characteristic of the MR fluid and causes problems for controllability. The relationship between damping performance and temperature must be defined in the control algorithms that control the absorber when used in a system such as structure, vehicle, and medical haptic. In this work, a new methodology has been presented to describe dynamic behaviours of MR absorber depending on temperature based on the Bouc-Wen model. Seven parameters in the Bouc-Wen model have been evaluated depending on temperature. Thus, damper force has been defined depending on temperature with a single equation that significantly simplifies the control process. When the experimental and the model results have been compared, it was shown that the error rates varied between %0.89 and %8.4. The average errors of the displacement, time and velocity have been 1.75%, 6.6%, and 4.4%, respectively.

1. INTRODUCTION

Magnetorheological (MR) fluids were discovered for the first time in the 1940s, but work on this subject has gained momentum since 1990. One of the devices that can be used with MR fluid is an absorber (damper), which is a vibration control system as semi active and has been attracting both scientists and technology companies in recent years due to its high vibration damping potentials. Semi active control systems are preferred because they have both the performance of active control systems and the simplicity of passive systems. However, the dynamic characterizations of MR damper still can not be fully explored today. MR dampers have a high viscous control range, relatively low power consumption, low cost, small size, and quick response [1].

Effective control of an MR damper to develop a control algorithm depends on understanding its non-linear behaviour [2]. The models of non-linear hysteresis behaviour are classified as non-parametric and parametric. The model parameters inside the non-parametric models don't requirement have physical meaning [3]. The models of Chebychev polynomials [4,5], Neural-Networks [6-9] and Neuro-Fuzzy [10,11] are some of the non-parametric models that can effectively represent the behaviour of MR dampers. However, it is widely known that models such as Neural-Networks and Neuro-Fuzzy require big data sets.

*Corresponding author, e-mail:zparlak@sakarya.edu.tr

The parameters in the parametric models representative any mechanical elements are determined based on the experimental data.

Stanway et al. [12] developed Bingham visco-plastic model for the force-displacement behaviour. However, it cannot model non-linear force-velocity response. Gamota and Filisko [13] proposed the Bingham visco-elastic-plastic model. Wereley et al. [14] proposed the non-linear biviscous model to improve the representation of the pre-yield hysteresis. Choi et al. [15] proposed showed polynomial model. In the model proposed by Dominguez et al. [16], the parameters of Bouc-Wen model were dependent on frequency, amplitude and current excitation. However, the temperature, which has an essential effect on the dynamic characteristic of MR damper was not one of these parameters. The Bouc-Wen model can predict non-linear force-velocity behaviour closely experimental data.

Some studies have been carried out to model MR devices behavior. Felt et al. [17] performed experimental tests on the behaviour of magnetic suspensions. These suspensions exhibited Newtonian flow in the absence of the magnetic field effect, whereas viscosity under the magnetic field increased markedly and exhibited non-Newtonian properties. Yasrebi et al. [18] compared the results of the electromagnetic analysis of finite element analysis with the manufactured MR damper and stated that the results are compatible with each other. Dyke S. et al. [19] conducted a study evaluating the proposed semi-active control algorithms for MR dampers. They stated that the control system performance depends on the choice of the semi-active control algorithms and that each semi-active control controller performs better than the passive control controllers. Dimock et al. [20] recommended the Bingham biplastic model and introduced non-dimensional terms to include additional parameters associated with the thickness fluid. Wereley and Pang [21] investigated damper performance by developing a quasi-static model for MR and electrorheological (ER) dampers for flow mode, mixed mode and slip mode. In the flow mode, it was indicated that the damping coefficient is a function of the number of core regions, in the mixed mode the field coefficient of the damping coefficient decreases when the field coefficient is large, and in the slip mode, the damping coefficient is only based on the Bingham number. Li and Du [22] experimentally investigated the rheological properties of the fluid for the MR brakes. They introduced a strengthening factor for their rotational speed that affects the brake performance of the magnetic field. It was stated that the boosting factor decreases with the rotation speed but increases with the magnetic field. Ellam et al. [23] examined the 2D isothermal and steady and behavior of Bingham plastic fluids between two plates with one moving and one stationary to measure flow cooling of the intelligent clutch. Wang and Gordaninejad [24] combined the Herschel-Bulkley constitutive equation and the fluids mechanistic-based approach to estimate the behaviour of MR and ER fluid dampers. The Herschel-Bulkley quasi-steady flow analysis included fluid compressibility for the non-linear dynamic behavior of the devices. Wereley [25] analyzed the damping capacity of controllable MR and ER damper under field-dependent exhibited post-yield shear thinning or thickening behaviour. A Herschel-Bulkley model with a field-dependent yield stress was offered and explained that the damping coefficient decreases for thinning fluids and increases for thickened fluids. Balamurugan et al. [26] developed the analytical characterization of MR damper using a new modified algebraic model, which requires less computation than the classical Bouc-Wen model. They found after tests that the new model worked in harmony with the full active suspension controller, except for minor distortions. Moradi N. et al. [27] developed a new modified Bouc-Wen model to characterize the behaviour of MR dampers. This new model included a hysteresis loop and showed more accurate results in the small speed range than the previous models.

There are also some studies on the behaviour of MR fluids and MR devices against temperature. However, these studies do not contribute to the development of control algorithms that can control an MR damper, taking into account the changing temperature effect. Mckee M. et al. [28] noted that while the temperature of MR fluid increased, the stiffness and energy dissipation decreased in their study. Priya and Gopalakrishnan [29] found that the temperature increased with a rising of input voltage and excitation frequency, affects energy dissipation capacity and MR damper force. Patel and Upadhyay [30] evaluated MR damper performance in terms of the thermo-rheological yields depending on temperature. Dong et al. [31] presented that MR absorber force can be reduced as the temperature is fluctuating based on the six σ robust optimal method. Priya and Gopalakrishnan [32] proposed PSO-GSA-SVR method to predict the hysteresis depending on temperature. Ferdous et. al. [1] presented a design technique to evaluate the temperature increase problem. Sherman et. al. [33] investigated the impacts of magnetic hysteresis and

noted that there was negligible increase at values of yield stress and no change at viscosity. Some recent studies [34- 37] on the relationship between MR damper and temperature have taken place in the literature. However, none of these coincide with the contribution presented in this study.

The overheating in the working conditions of the MR damper due to magnetic field and friction of moving parts changes seriously the characteristic of the MR fluid and causes severe controllability problems due to the control algorithms that do not take into account the temperature effect. This study has presented a new methodology to describe dynamic behaviours depending on temperature based on Bouc-Wen model as a novelty in the literature. Thus, the damper force has been de-fined depending on temperature with a single equation to control comfortably and more stable the MR damper when used in a system such as structure, vehicle, and medical haptic. The results of the model have been compared with the experimental data, and the errors have been calculated.

2. DESIGN OF THE MR DAMPER

The technology associated with vibration control is used in a vast field nowadays. Dampers with better performance in optimum design are required in all structures and mechanisms. The MR damper has a strong high pressure applied by the piston and the MR fluid flows from the narrow downstream channel to the lower pressure side. During the flow of the MR liquid from the channel, a magnetic field is applied to the liquid through the coil in the head of the piston. The iron particles in the MR liquid pass through the channel by the effect of the applied magnetic field and form a chain structure perpendicular to the flow (Figure 1). Due to this resistance, the apparent viscosity of the MR fluid increases. With the rise of the magnetic field applied to the MR fluid, the flow stress of the fluid will also increase.

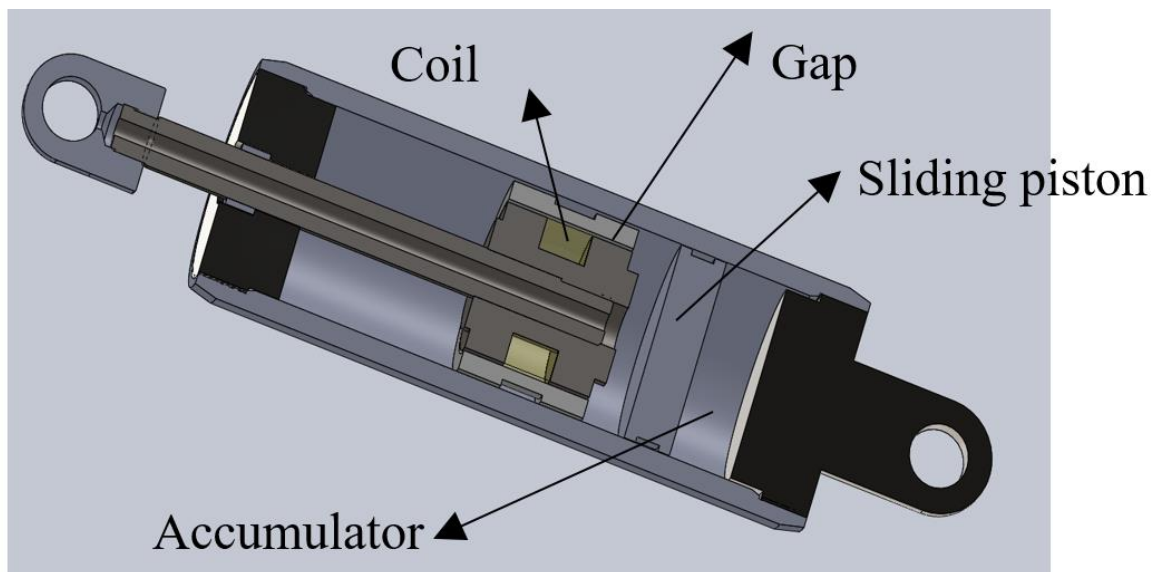


Figure 1. The schematic view of the MR damper

The essential components of MR damper are coil, hydraulic cylinder, piston rod, accumulator, piston head, upper and lower ends of hydraulic cylinder and MR fluid. The material of MR damper is chrome-plated steel for the piston rod and St37 steel for the other parts.

There are basically three types of MR dampers. They are divided into single-tube, double-tube and double-ended MR dampers. The most commonly used MR damper type is the one-tube MR damper. The reason is that it is being installed in any direction. There is only one pressurized gas reservoir for the accumulator in the single-tube MR damper. In a double-tube MR damper, there are two interiors of the tube, inner and outer tubes. A base valve is used to control the flow through the two liquid reservoirs. In the case of a double-ended MR damper, there are piston shafts with equal diameters on both sides of the MR damper, so this type of damper is called double-ended MR damper type [38].

The geometrical dimensions of the MR damper used at experiments of the study is shown in Figure 2.

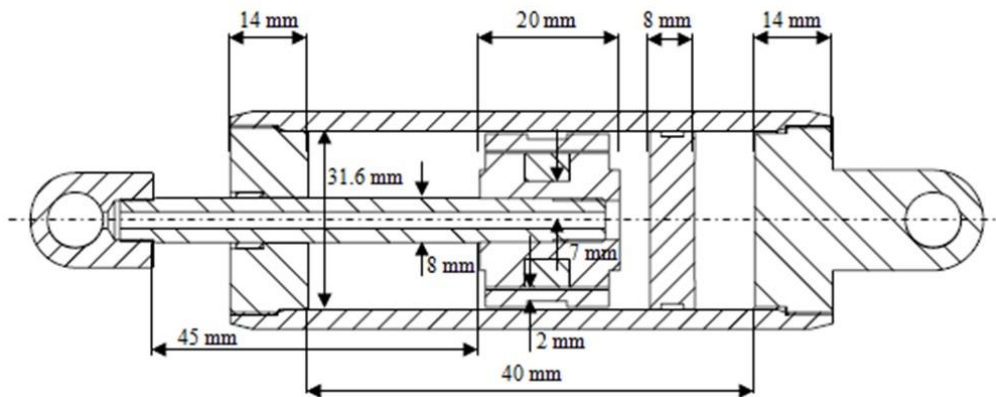


Figure 2. The dimensions of the MR damper

In addition, gap width, which is not specified on Figure 2, is 0.4mm. The coil width is 5.1 mm, and the number of turn of the coil is 120.

3. MODELLING OF HYSTERESIS BEHAVIOUR OF MR DAMPER

The models of MR dampers can be classified into two main categories. One of them is a quasi-static flow model, and the other is a dynamic model. The force-displacement characteristic can be described with the Bingham plastic model from quasi-static flow models. However, it is not sufficient for describing force-velocity characterization with a high hysteresis. The Bouc-Wen model gives the most accurate results in many proposed models for force-velocity characteristics [16, 27].

3.1. Temperature-Dependent Bouc-Wen Model

The rheological behaviours of the MR fluid [39] under applied constant currents, and temperature 20 °C to 70 °C were investigated with the rheometer of Anton Paar MCR 302 (Figure 3). Temperature change versus the change in yield stress, which causes the change in the fluid's viscosity, is given in Figure 4. These changes affect the operation of the MR damper. Therefore, it is essential to see the effect of the temperature on performance.

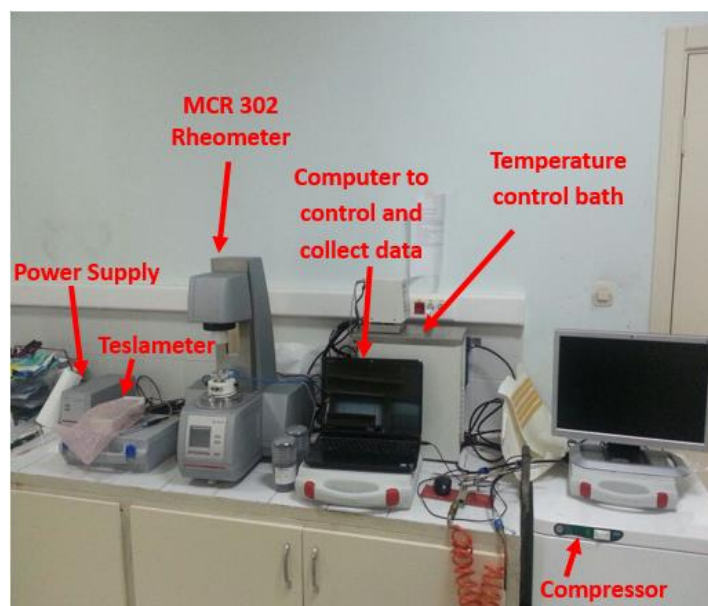


Figure 3. Anton Paar MCR 302 rheometer test set-up

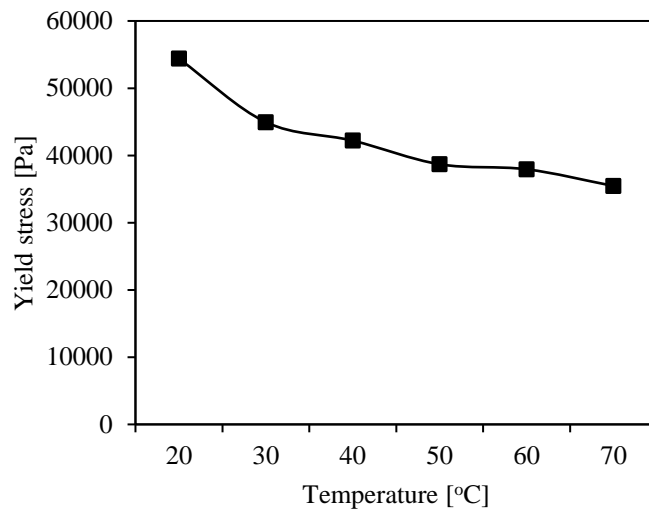


Figure 4. Change of yield stress of MRF132 with temperature

The damper tests at various temperatures to examine the performance under 1A. 24.6% performance loss is depicted in Figure 5, which indicates the importance of changing temperature. The control algorithms should be considered this effect in its developing process.

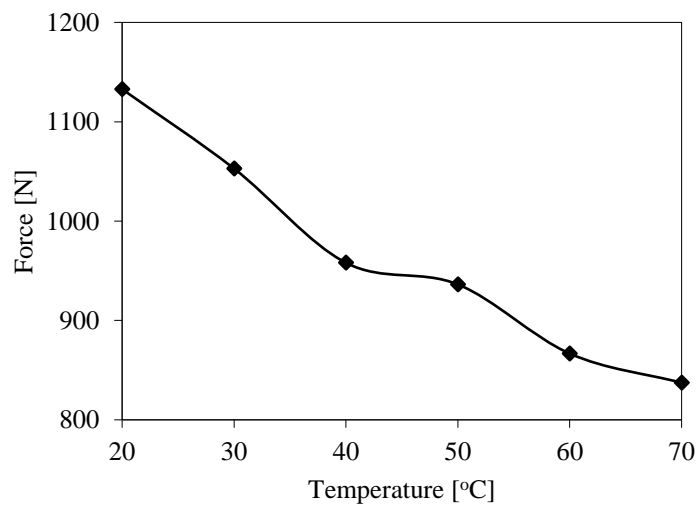


Figure 5. Change of damper force with temperature

The mathematical representation of the Bouc-Wen model is given in Figure 6. It consists of a spring, a damping element and a representation of the Bouc-Wen hysteresis.

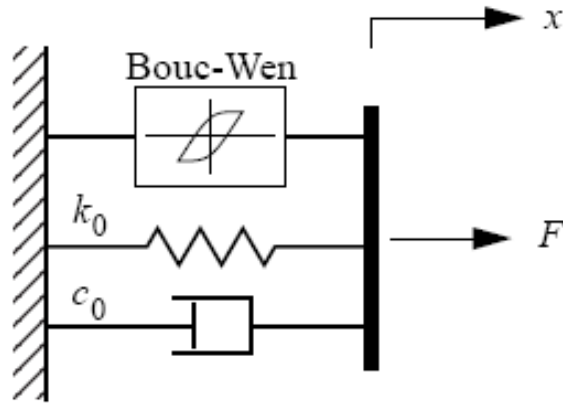


Figure 6. Bouc-Wen model

The total force equation for the classical Bouc-Wen model is given below

$$f = c_0 \dot{x} + k_0 x + \alpha z \quad (1)$$

where x and \dot{x} is displacement and velocity of the damper, respectively. c_0 is the damping coefficient, k_0 is the spring stiffness, and z is the dimensionless hysteresis variable and is defined as a first-order differential equation

$$\dot{z} = -\gamma |\dot{x}| |z|^{(n-1)} z - \beta \dot{x} |z|^n + A \dot{x}. \quad (2)$$

The total force is affected by seven variables, which are c_0 , k_0 , α , γ , β , n , and A . Equation (2) can be expressed as follows:

$$\frac{dz}{dx} = A - ((\beta + \gamma \text{sgn}(\dot{x}z))) |z|^n \quad (3)$$

where sgn represents the signum function. Solving Equation (3). It was concluded by Spencer [40] that as n increases, the curvature radius decreases in the vicinity of the transition velocity points in which the force increases exponentially in the positive and negative direction with velocity on force-velocity curve. It was considered $n = 2$ by studies [2, 15, 16, 41] and Equation (3) can be solved analytically as following;

$$z = \frac{\sqrt{A}}{\sqrt{(\beta+\gamma)}} \tanh(\sqrt{A(\beta+\gamma)}(\dot{x} + C)) \quad (4)$$

where C is the integration constant and is derived from boundary conditions. The evolutionary force, $f_z = \alpha z$ in Equation (1) and $f_z = f_{z0}$ at $\dot{x} = 0$ yields;

$$C = \frac{1}{\sqrt{A(\beta+\gamma)}} \operatorname{atanh}\left(\frac{\pm f_{z0} \sqrt{(\beta+\gamma)}}{\alpha \sqrt{A}}\right). \quad (5)$$

Thus the total force is;

$$f = c_0(a\omega \cos(\omega t)) + k_0(asin(\omega t)) + \alpha \left\{ \frac{\sqrt{A}}{\sqrt{(\beta+\gamma)}} \tanh\left(\sqrt{A(\beta+\gamma)}(\dot{x} + \frac{1}{\sqrt{A(\beta+\gamma)}} \operatorname{atanh}\left(\frac{\pm f_{z0} \sqrt{(\beta+\gamma)}}{\alpha \sqrt{A}}\right))\right) \right\} \quad (6)$$

ω is the angular frequency of the piston head, and a is the half stroke of the damper. As seen from Equation (6), the damper force is analytically expressed.

4. EXPERIMENTAL STUDY

MR damper was filled with MRF-132DG [39], a commercial liquid produced by LORD company, in a volume of about 50 mm³. In addition, nitrogen gas was compressed into the accumulator part in the MR damper at the pressure of 20 bar so that there is no air space in the dampers.

The test setup consisted of a damper test machine, computer, heat sink and power supply, shown in Figure 7 in the laboratory of Applied Fluids in Mechanical Engineering of Sakarya University. The damper test machine is Roehrig MK-2150. The load cell of Interface 1210Af-5K-B to measure damping force, its maximum capacity is 22 kN, and a linear variable displacement transducer of Trans-Tek 0122-0001 is used to measure displacement. The temperature from absorber outside surface was measured by sensors of Raytek RAY CI. The power supply of GWinstek PPE 3223 fed current into the MR damper. A temperature controlled heat sink bath kept the temperature at the desired level. The SHOCK 6.3 computer software controlled the test machine and collected the test data. These tests were carried out under a constant current of 1A and with a constant frequency of 0.4 1/s. A heat sink (temperature control bath) shown in Figure 7, was used to provide the desired temperature of damper.

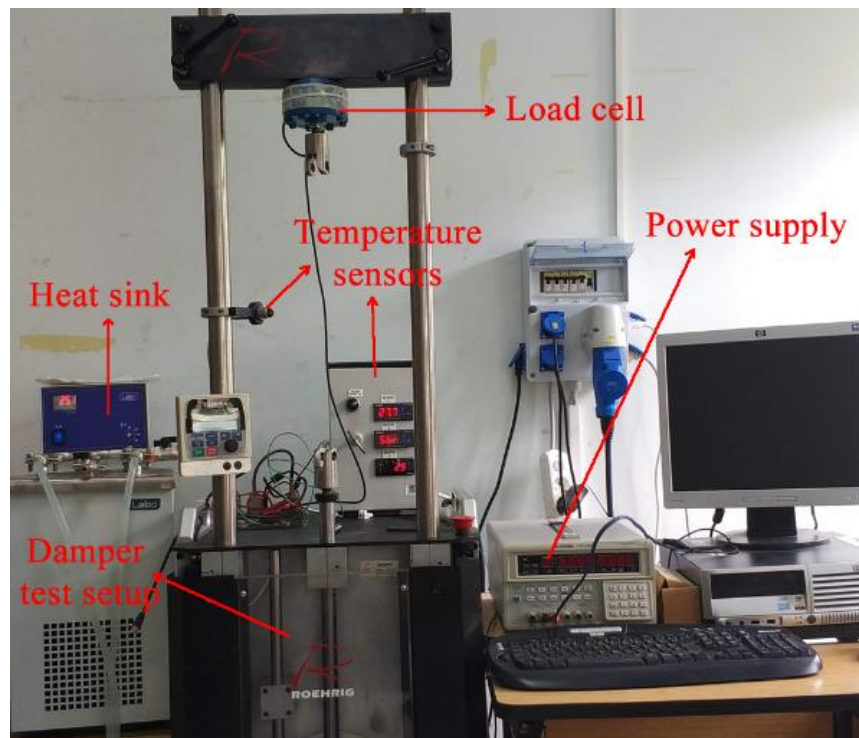


Figure 7. Test Setup

5. RESULTS AND DISCUSSIONS

5.1. The Dynamic Model Validation

The relationship between the seven parameters in Equation (6) and temperature was determined by regression analysis using experimental data, which is the relationship of force-time for each temperature, performed at 20°C, 30°C, 40°C, 50°C, 60°C and 70°C. By fitting Equation (6) to the experimental data, the value of the parameters in Equation (6) was obtained for each temperature. The curves formed by these values for each temperature are given in Figure 8. (The values of parameter c_0 were divided into 10 to provide all curves within the same scale.)

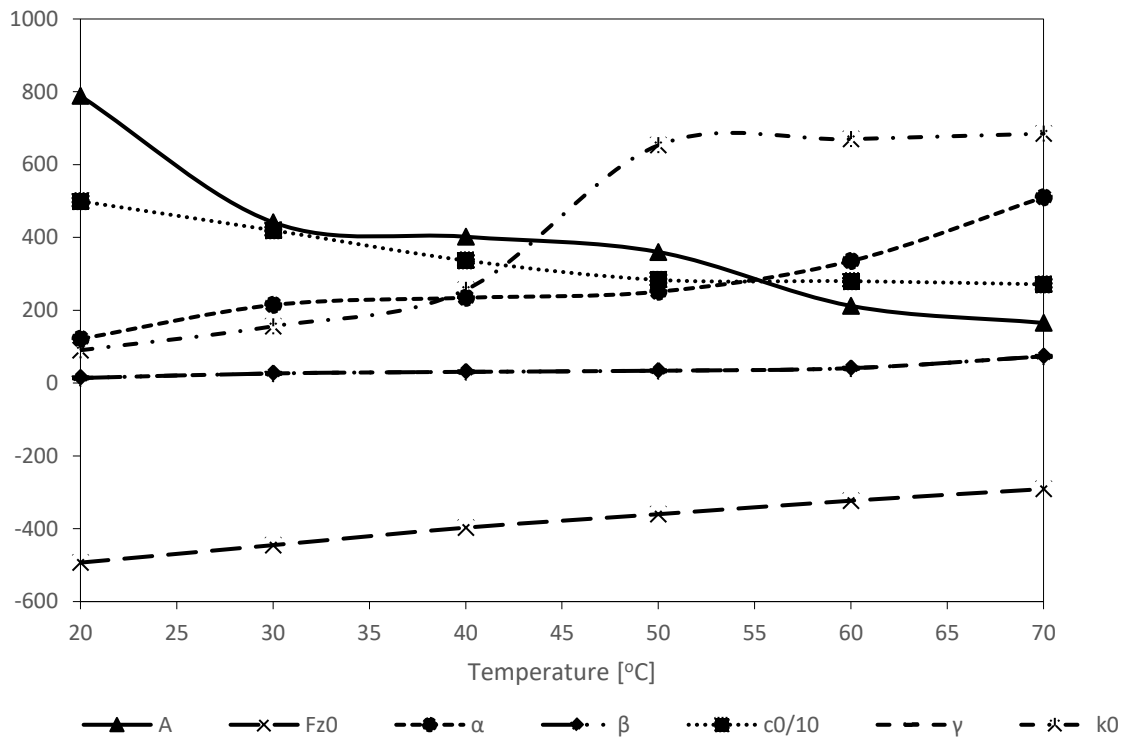


Figure 8. The relationships between temperature and α , β , γ , A , c_0 , k_0 , f_{z0}

It was seen that the most sensitive parameter to temperature change is c_0 . Also, γ and β are nearly at the same values, and they were the most insensitive parameters to temperature.

A temperature-dependent equation was fitted to each of the change curves of these parameters in Figure 8. The parameters tend to vary exponentially with the temperature. Equations (7)-(13) shows the relationship of each of these parameters to temperature. In addition, the determination coefficients of each curve is given in Equations (7)-(13)

$$c_0(T) = c_{01} \left(1 + e^{\frac{c_{02}}{T}} \right) \quad R^2=0.9412 \quad (7)$$

$$k_0(T) = k_{01} e^{-\left(\frac{T-k_{02}}{k_{03}} \right)} \quad R^2=0.955 \quad (8)$$

$$\alpha(T) = \alpha_1 e^{\alpha_2 * T} + \alpha_3 \quad R^2=0.9566 \quad (9)$$

$$\gamma(T) = \gamma_1 e^{\gamma_2 * T} + \gamma_3 \quad R^2=0.9432 \quad (10)$$

$$\beta(T) = \beta_1 e^{\beta_2 * T} + \beta_3 \quad R^2=0.9432 \quad (11)$$

$$A(T) = A_1 (1 + e^{-T}) \quad R^2= 0.9392 \quad (12)$$

$$f_{z0}(T) = f_{z01} e^{f_{z02} * T} \quad R^2= 0.9997. \quad (13)$$

Figure 9 shows an exponential and linear regression of parameter c_0 . It is seen that exponential fitting provides a much better correlation.

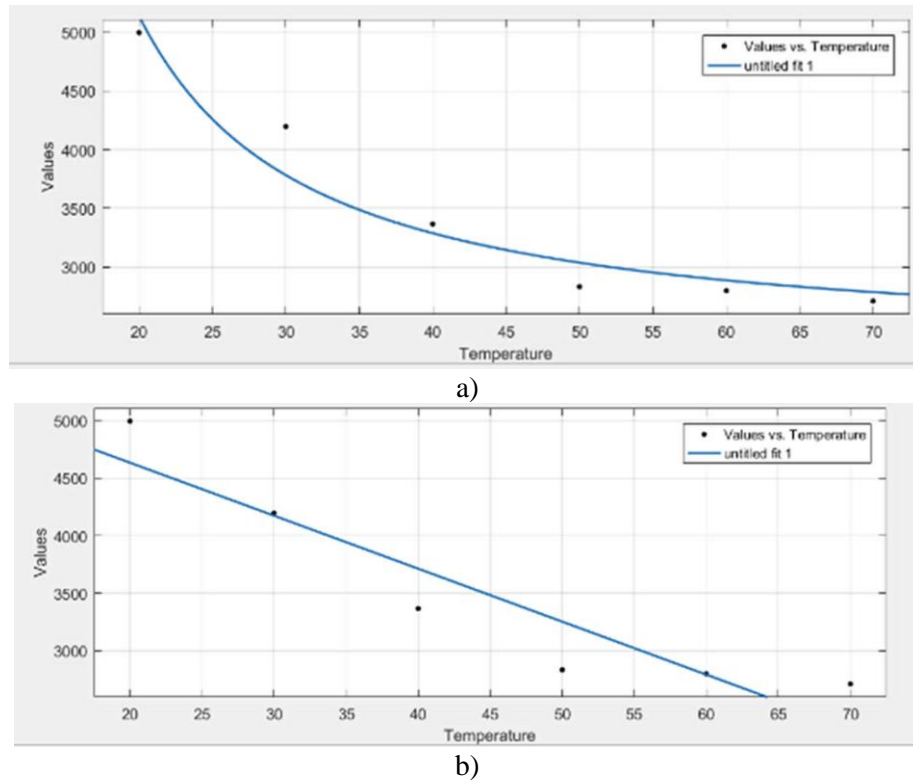


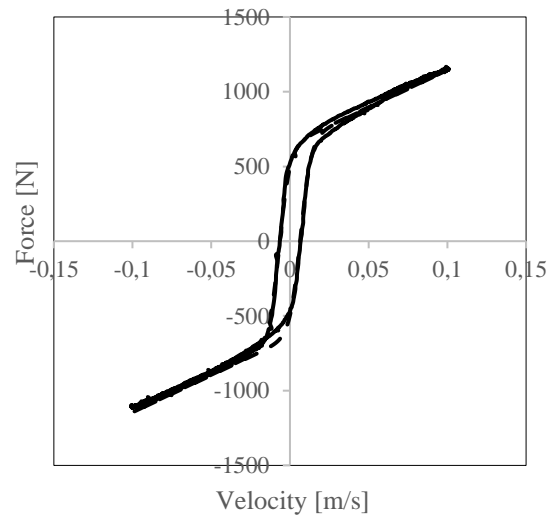
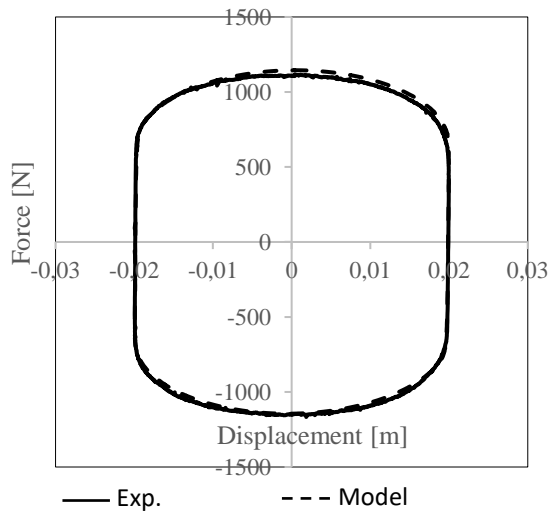
Figure 9. Regression analysis for c_0 a) exponential b) linear

In Equations (7)-(13) the values of constant parameters of A_1 , f_{z01} , f_{z02} , α_1 , α_2 , α_3 , β_1 , β_2 , β_3 , c_{01} , c_{02} , γ_1 , γ_2 , γ_3 , k_{01} , k_{02} and k_{03} should be estimated, determined or explicitly measured for the MR damper used in a system.

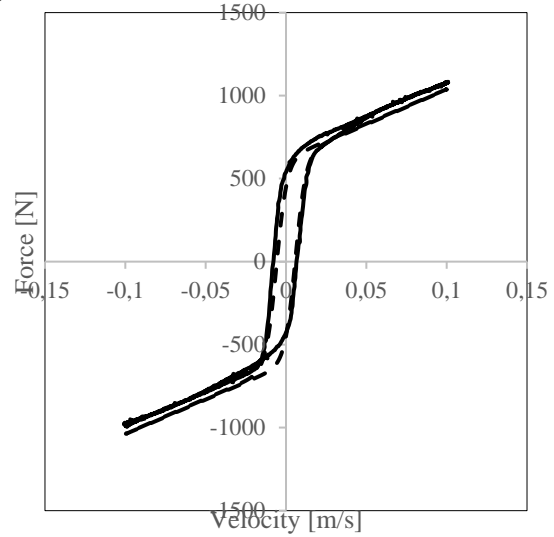
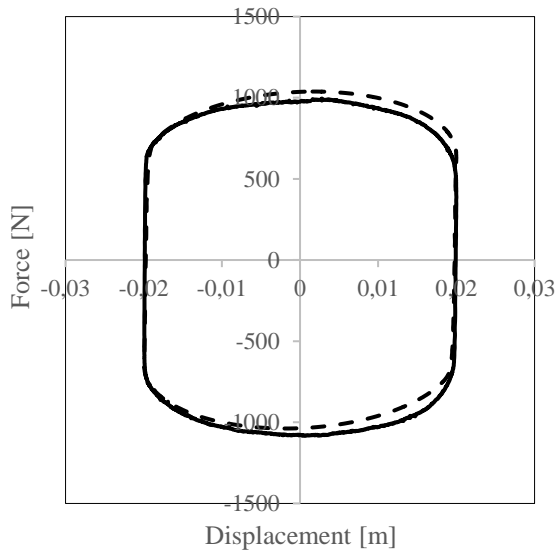
When Equations (7)-(13) is substituted into Equation (6), the damper damping force is obtained depending on temperature.

Equation (1), a closed-state differential equation because of its hysteresis variable, was transformed into an algebraic function based on temperature. This equation can be used to estimate the changing damping force under the influence of temperature generated by an MR damper by providing the coefficients. This equation would be adapted easily to the control algorithms considered the temperature effect on the damping force.

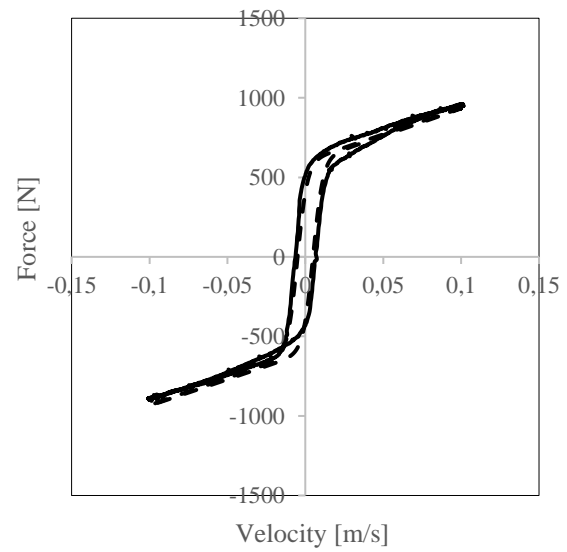
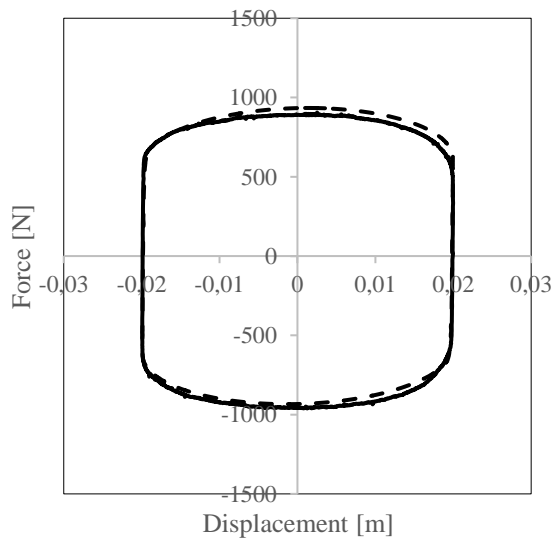
Comparing the results between the Bouc-Wen model from Equation (6) (with substituting Equations (7)-(13) and the experimental under different temperatures is shown at Figure 10.



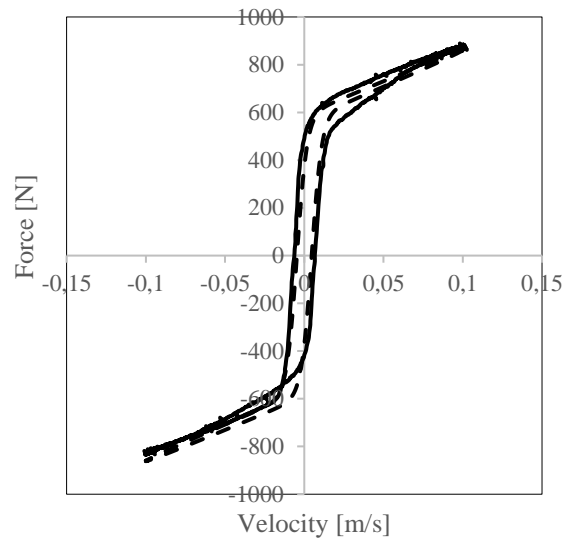
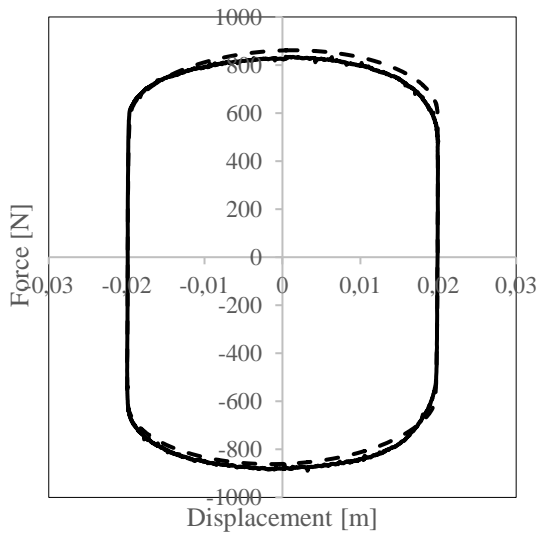
a)



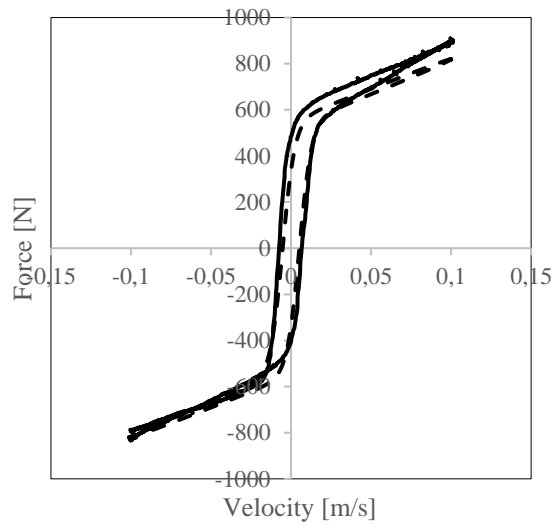
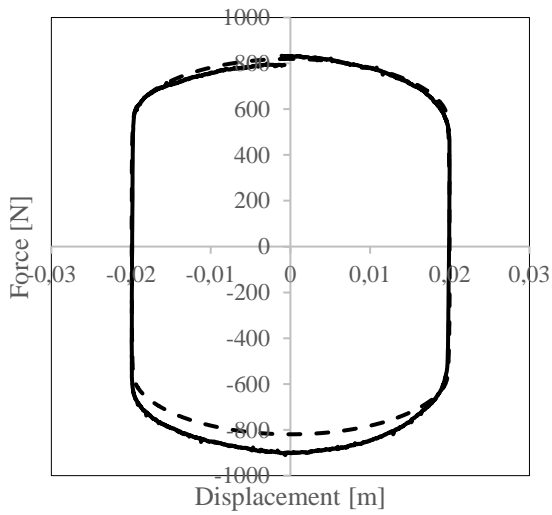
b)



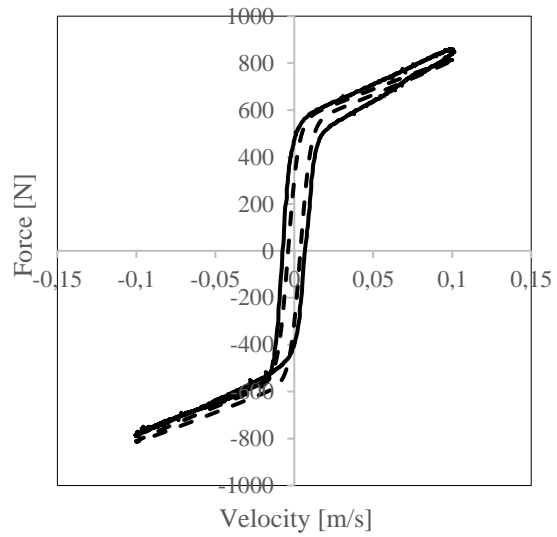
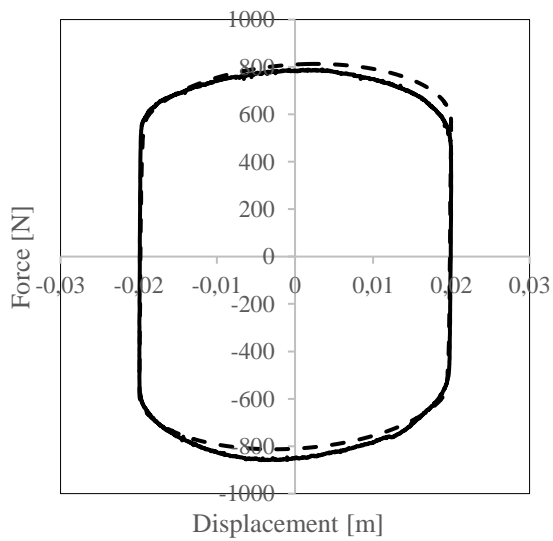
c)



d)



e)



f)

Figure 10. Force-Displacement and Force-Velocity graphs for (a) 20°C, (b) 30°C, (c) 40°C, (d) 50°C, (e) 60°C, (f) 70°C

As can be seen once again on Figure 10, the damper force decreases with increasing temperature. It may cause not generate the required damping force of MR damper. Furthermore, as seen in Figure 10, there is a good agreement between the experimental data and the Bouc-Wen model results. The model can characterize the hysteresis behaviour in force-velocity. Plus to this graphical proof, a quantitative error analysis was made.

5.2. Error Analysis

The quantitative error analysis between the experimental data and the model were done as a function of displacement (E_x), velocity ($E_{\dot{x}}$) and time (E_t), which was given by Spencer et al. [2] as

$$E_t = \sqrt{\frac{\int_0^t (F_e - f)^2 dt}{\int_0^t (F_e - F_o)^2 dt}} \quad (14)$$

$$E_x = \sqrt{\frac{\int_0^t (F_e - f)^2 \left| \frac{dx}{dt} \right| dt}{\int_0^t (F_e - F_o)^2 dt}} \quad (15)$$

$$E_{\dot{x}} = \sqrt{\frac{\int_0^t (F_e - f)^2 \left| \frac{d\dot{x}}{dt} \right| dt}{\int_0^t (F_e - F_o)^2 dt}} \quad (16)$$

where, the f is force calculated by the Equation (6) (with substituting Equations (7)-(13) , F_e is the experimental force, and F_o is the mean value of experimental force for one cycle of the MR damper. The results of the error analysis can be seen in Table 1.

Table 1. Results of the error analysis

Temperature [°C]	E_t [%]	E_x [%]	$E_{\dot{x}}$ [%]
20	6.961	1.003	4.712
30	7.765	2.078	5.351
40	5.886	1.415	3.804
50	4.744	0.895	2.842
60	8.420	3.136	5.655
70	6.305	1.978	4.250

In the error analysis, the lowest value was 0.89%, it is the displacement error for 50 °C, and the biggest value was 8.42%, it is the time error of 60 °C. The average errors of the displacement, time and velocity were 1.75%, 6.6% and 4.4%, respectively. The lowest average error according to temperature occurred as 2.8% at 50 °C.

6. CONCLUSIONS

Hysteresis behaviours of MR dampers observed in force-velocity curves can be captured by creating a new dynamic model, such as Bouc-Wen model. This dynamic model has an essential place in the control applications. Parlak et al. [38] the dynamic model of MR damper was determined depending on current excitation. In this study, the dynamic behaviour of the damper was modelled by considering the temperature effect based on Bouc-Wen model, the dynamic behaviours were modelled against all possible situations of MR damper to develop a control algorithm.

The seven variable parameters in the Bouc-Wen model were transformed into a form that depends only on the temperature change as an algebraic equation. The results of the new model were compared with the experimental results. It was observed that both force-displacement and force-velocity curves are highly compatible with the results of the experimental. According to the error analysis results, error rates varied between %0.89 and %8.4. The average errors at different temperatures ranged from 2.83% to 5.74%. The average errors depart from time, displacement, and velocity are 6.68%, 1.75% and 4.44%, respectively.

Therefore, a new methodology was developed to describe the dynamic characterization of an MR damper with temperature in this study. The same methodology can also be adapted to another MR damper to obtain parameters in Equation (6). Thus, it is possible to safely use a single equation, which is a function of temperature, to control the behaviour of the MR damper depending on the temperature.

CONFLICTS OF INTEREST

No conflict of interest was declared by the authors.

REFERENCES

- [1] Ferdaus, M. M., Rashid, M. M., Hasan, M. H., Yosuf, H. B. M., Bhuiyan, M. M. I., Alraddadi, A., “Temperature effect analysis on magnetorheological damper’s performance”, *Journal of Automation and Control Engineering* 2(4): 392-396, (2014).
- [2] Spencer, B. F., Dyke, S. J., Sain, M. K., Carlson, J. D., “Phenomenological model of a magnetorheological damper”, *Journal of Engineering Mechanics-ASME*, 123(3): 230–238, (1997).
- [3] Boada, M. J. L., Calvo, J. A., Boada, B. L., Díaz, V., “Modeling of a magnetorheological damper by recursive lazy learning”, *International Journal of Non-Linear Mechanics*, 46(3): 479-485, (2011).
- [4] Ehr Gott, R. C., Masri, S. F., “Modeling the oscillatory dynamic behaviour of electrorheological materials in shear”, *Smart Materials and Structures*, 1(4): 275–285(1992).
- [5] Gavin, H. P., Hanson, R. D., Filisko, F. E., “Electrorheological dampers, Part II: testing and modeling”, *Journal of Applied Mechanics*, 63: 676–682, (1996).
- [6] Chang, C. C., Roschke, P., “Neural network modeling of a magnetorheological damper”, *Journal of Intelligent Material Systems and Structures*, 9(9): 755–764, (1998).
- [7] Chang, C. C., Zhou, L., “Neural network emulation of inverse dynamics for a magnetorheological damper”, *Journal of Structural Engineering*, 128(2): 231–239, (2002).
- [8] Wang, D. H., Liao, W. H., “Modeling and control of magnetorheological fluid dampers using neural networks”, *Smart Materials and Structures*, 14(1): 111–126, (2004).
- [9] Du, H., Lam, J., Zhang, N., “Modelling of a magnetorheological damper by evolving radial basis function networks”, *Engineering Applications of Artificial Intelligence*, 19(8): 869–881, (2006).
- [10] Schurter, K. C., Roschke, P. N., “Fuzzy modeling of a magnetorheological damper using ANFIS”, *Proceedings of IEEE International Conference on Fuzzy Systems*, San Antonio, TX, USA, 1: 122–127, (2000).
- [11] Wilson, C. M. D., Abdullah, M. M., “Structural vibration reduction using fuzzy control of magnetorheological dampers” In *Structures Congress 2005: Metropolis and Beyond*, New York, USA, 1: 1-12, (2005).
- [12] Stanway, R., Sproston, J. L., Stevens, N. G., “Non-linear modelling of an electrorheological vibration damper”, *Journal of Electrostatics*, 20(2): 167–184, (1987).
- [13] Gamota, D. R., Filisko, F. E., “Dynamic mechanical studies of electrorheological materials: moderate frequencies”, *Journal of Rheology*, 35(3): 399-425, (1991).

- [14] Wereley, N. M., Pang, L., Kamath, G. M., “Idealized hysteresis modeling of electrorheological and magnetorheological dampers”, *Journal of Intelligent Material Systems and Structures*, 9(8): 642-649, (1998).
- [15] Choi, S. B., Lee, S. K., Park, Y. P., “A hysteresis model for the field-dependent damping force of a magnetorheological damper”, *Journal of Sound and Vibration*, 245(2): 375–383, (2001).
- [16] Dominguez, A., Sedaghati, R., Stiharu, I., “A new dynamic hysteresis model for magnetorheological dampers”, *Smart Material and Structure*, 15(5): 1179–1189, (2006).
- [17] Felt, D. W., Hagenbuchle, M., Liu, J., Richard, J., “Rheology of a magnetorheological fluid”, *Journal of Intelligent Material Systems and Structures*, 7(5): 589-593, (1996).
- [18] Yasrebi, N., Ghazavi, A., Mashhadi, M. M., Yousefi-Koma, A., “Magnetorheological fluid dampers modeling: Numerical and experimental”, In *Proceeding of the 17th IASTED international conference modeling and, simulation*, Isfahan, Iran, 1: (1-6), (2006).
- [19] Dyke, S. J., Spencer, B. F., “A comparison of semi-active control strategies for the MR damper”, *IEEE In Intelligent Information Systems*, Grand Bahama Island, Bahamas, 1: 580-584, (1997).
- [20] Dimock, G. A., Lindler, J. E., Wereley, N. M., “Bingham biplastic analysis of shear thinning and thickening in magnetorheological dampers”, *SPIE's 7th Annual International Symposium on Smart Structures and Materials*, Newport Beach, CA, United States, 3985: 444-456, 2000.
- [21] Wereley, N. M., Pang, L., “Nondimensional analysis of semi-active electrorheological and magnetorheological dampers using approximate parallel plate models”, *Smart Materials and Structures*, 7(5): 732-743, (1998).
- [22] Li, W. H., Du, H., “Design and experimental evaluation of a magnetorheological brake”, *The International Journal of Advanced Manufacturing Technology*, 21(7): 508-515, (2003).
- [23] Ellam, D. J., Atkin, R. J., Bullough, W. A., “Analysis of a smart clutch with cooling flow using two-dimensional Bingham plastic analysis and computational fluid dynamics”, *Proceedings of the Institution of Mechanical Engineers, Part A: Journal of Power and Energy*, 219(8): 639-652, (2005).
- [24] Wang, X., Gordaninejad, F., “Flow analysis and modeling of field-controllable, electro-and magnetorheological fluid dampers”, *Journal of Applied Mechanics*, 74(1): 13-22, (2007).
- [25] Wereley, N. M., “Nondimensional Herschel—Bulkley analysis of magnetorheological and electrorheological dampers”, *Journal of Intelligent Material Systems and Structures*, 19(3): 257-268, (2008).
- [26] Balamurugan, L., Jancirani, J., Eltantawie, M. A., “Generalized magnetorheological (MR) damper model and its application in semi-active control of vehicle suspension system”, *International Journal of Automotive Technology*, 15(3): 419-427, (2014).
- [27] Moradi Nerbin, M., Mojed Gharamaleki, R., Mirzaei, M., “Novel optimal control of semi-active suspension considering a hysteresis model for MR damper”, *Transactions of the Institute of Measurement and Control*, 39(5): 698-705, (2017).
- [28] McKee, M., Gordaninejad, F., Wang, X., “Effects of temperature on performance of compressible magnetorheological fluid suspension systems”, *Journal of Intelligent Material Systems and Structures*, 29(1): 41-51, (2018).

- [29] Priya, C. B., Gopalakrishnan, N., “Experimental Investigations of the Effect of Temperature on the Characteristics of MR Damper”, In Recent Advances in Structural Engineering, Singapore, 2: 435-443, (2018).
- [30] Patel, D. M., Upadhyay, R. V., “Predicting the thermal sensitivity of MR damper performance based on thermo-rheological properties”, Materials Research Express, 6(1): 015707, (2018).
- [31] Dong, X., Yu, J., Wang, W., Zhang, Z., “Robust design of magnetorheological (MR) shock absorber considering temperature effects”, The International Journal of Advanced Manufacturing Technology, 90(5-8): 1735-1747, (2017).
- [32] Priya, C. B., Gopalakrishnan, N., “Temperature dependent modelling of magnetorheological (MR) dampers using support vector regression”, Smart Materials and Structures, 28(2): 025021, (2019).
- [33] Sherman, S. G., Powell, L. A., Becnel, A. C., Wereley, N. M., “Scaling temperature dependent rheology of magnetorheological fluids”, Journal of Applied Physics, 117(17): 17C751, (2015).
- [34] Liang, G., Zhao, T., Li, N., Wei, Y., Savaresi, S. M., “Magnetorheological damper temperature characteristics and control-oriented temperature-revised model”, Smart Materials and Structures, 30(12): 125005, (2021).
- [35] Du, C., Zeng, F., Liu, B., Fu, Y., “A novel magnetorheological fluid damper with a heat insulation function”, Smart Materials and Structures, 30(7): 075001, (2021).
- [36] Savaia, G., Corno, M., Panzani, G., Sinigaglia, A., Savaresi, S. M., “Temperature Estimation in a Magneto-Rheological Damper”, In 2020 IEEE Conference on Control Technology and Applications, CCTA, 1: 567-572, (2021).
- [37] Jastrzębski, Ł., Sapiński, B., Koziel, A., “Automotive mr shock absorber behaviour considering temperature changes: experimental testing and analysis. acta mechanica et automatic”, 14(1), (2020).
- [38] Parlak, Z., Engin, T., Çeşmeci, Ş., Şahin, İ., “Dynamic characterization of a vehicle magnetorheological damper”, International Journal of Vehicle Design, 59(2/3): 129-146, (2012).
- [39] Lord Corporation, “MRF-132DG Magneto-Rheological Fluid”, http://www.lordmrstore.com/_literature_231215/Data_Sheet_-_MRF-132DG_Magneto-Rheological_Fluid, (2021).
- [40] Spencer, B. F. Jr., “Reliability of Randomly Excited Hysteretic Structures”, Berlin: Springer, 21: 77-93, (1986).
- [41] Yao, G. Z., Yap, F. F., Chen, G., Li, W., Yeo, S. H., “MR damper and its application for semi-active control of vehicle suspension system”, Mechatronics, 12(7): 963-973, (2002).